
Relationship Between ^{18}F -FDG PET/CT Scans and *KRAS* Mutations in Metastatic Colorectal Cancer

Kenji Kawada*¹, Kosuke Toda*¹, Yuji Nakamoto², Masayoshi Iwamoto¹, Etsuro Hatano¹, Fengshi Chen³, Suguru Hasegawa¹, Kaori Togashi², Hiroshi Date³, Shinji Uemoto¹, and Yoshiharu Sakai¹

¹Department of Surgery, Graduate School of Medicine, Kyoto University, Kyoto, Japan; ²Department of Diagnostic Imaging and Nuclear Medicine, Graduate School of Medicine, Kyoto University, Kyoto, Japan; and ³Department of Thoracic Surgery, Graduate School of Medicine, Kyoto University, Kyoto, Japan

Several studies have shown that *KRAS* mutations in colorectal cancer (CRC) result in the lack of response to anti-epidermal growth factor receptor–based therapy; thus, *KRAS* mutational testing has been incorporated into routine clinical practice. However, 1 limitation of this test is the heterogeneity of *KRAS* status, which can be either intratumoral heterogeneity within an individual primary CRC or discordant *KRAS* status between a primary CRC and its corresponding metastases. We previously reported that ^{18}F -FDG accumulation was significantly higher in primary CRCs with mutated *KRAS* than in those with wild-type *KRAS*. However, the clinical utility of the previous report has been limited because endoscopic biopsy for testing *KRAS* status is safe and feasible only in primary CRC. The purpose of this study was to investigate whether *KRAS* status is associated with ^{18}F -FDG accumulation in metastatic CRC and whether ^{18}F -FDG PET/CT scans can be used to predict the *KRAS* status of metastatic CRC. **Methods:** A retrospective analysis was performed on 55 metastatic CRC tumors that were identified by ^{18}F -FDG PET/CT before surgical resection. Maximum standardized uptake value (SUV_{max}) of the respective metastatic tumor was calculated from ^{18}F -FDG accumulation. **Results:** From the analysis with the 55 tumors, no significant correlation was found between SUV_{max} and *KRAS* status. We next analyzed only tumors larger than 10 mm to minimize the bias of partial-volume effect and found that SUV_{max} was significantly higher in the *KRAS*-mutated group than in the wild-type group (8.3 ± 4.1 vs. 5.7 ± 2.4 , respectively; $P = 0.03$). Multivariate analysis indicated that SUV_{max} remained significantly associated with *KRAS* mutations ($P = 0.04$). *KRAS* status could be predicted with an accuracy of 71.4% when an SUV_{max} cutoff value of 6.0 was used. **Conclusion:** ^{18}F -FDG accumulation into metastatic CRC was associated with *KRAS* status. ^{18}F -FDG PET/CT scans may be useful for predicting the *KRAS* status of metastatic CRC and help in determining the therapeutic strategies against metastatic CRC.

Key Words: metastatic colorectal cancer; genetics; *KRAS*; ^{18}F -FDG PET/CT; imaging

J Nucl Med 2015; 56:1322–1327

DOI: 10.2967/jnumed.115.160614

Colorectal cancer (CRC) develops through accumulation of genetic alterations in oncogenes and tumor suppressors. Mutations in the *KRAS* gene occur in approximately 40% of CRCs and involve codons 12 and 13 in more than 90% cases. Several studies have shown that *KRAS* mutations predict a lack of response to therapies targeted to the epidermal growth factor receptor (EGFR) (1,2). The anti-EGFR monoclonal antibodies cetuximab and panitumumab are currently recommended to use only for CRC tumors with wild-type *KRAS*, although a wild-type *KRAS* does not guarantee a response to either antibody. *KRAS* mutational testing of primary CRC samples has been incorporated into routine clinical practice for the purpose of treatment algorithms. However, 1 limitation of *KRAS* mutational testing is the heterogeneity of *KRAS* status, which can be either intratumoral heterogeneity within an individual primary CRC (3) or discordant *KRAS* status between a primary CRC and its corresponding metastases (4,5). Another limitation is failure to determine *KRAS* mutational status due to poor DNA quality of biopsy samples. In addition, mutational testing requires tumor tissue samples resected by biopsy or surgery, but the samples from metastatic tumors are usually difficult to access and may need invasive procedures.

PET/CT with ^{18}F -FDG is used to evaluate glucose metabolism by measuring uptake of ^{18}F -FDG, a glucose analog. This is a less invasive tool for diagnosis, treatment response monitoring, surveillance, and prognostication of CRC. ^{18}F -FDG is transported into cells via glucose transporters (GLUTs) and then phosphorylated by hexokinases to FDG-6-phosphate, which becomes trapped within the cells. In most types of cancers, ^{18}F -FDG accumulation depends largely on the glucose transporter-1 (GLUT1) and the rate-limiting glycolytic enzyme hexokinase type 2 (6). For CRC, several recent studies have suggested that GLUT1-mediated ^{18}F -FDG accumulation is more essential than hexokinase activity (6). It was previously reported that in CRC cell lines, under normoxic conditions, the increase in GLUT1 expression and glucose uptake is critically dependent on *KRAS* mutations (7). Using human clinical samples, we previously reported that *KRAS* mutations significantly increased ^{18}F -FDG accumulation into primary CRC possibly through upregulation of GLUT1 expression but not hexokinase type 2 expression (8). Hypoxia-inducible factor-1 α (HIF-1 α) is a transcriptional factor that mediates cellular response to hypoxia, including angiogenesis and glucose metabolism. In hypoxic cells, HIF-1 α enhances glycolysis by inducing glucose transporter and several enzymes involved in glycolysis (9). In both in vitro and in vivo animal experiments, we recently showed that mutated *KRAS*

Received May 8, 2015; revision accepted Jun. 18, 2015.

For correspondence or reprints contact: Kenji Kawada, Department of Surgery, Graduate School of Medicine, Kyoto University, 54 Shogoin-Kawara-cho, Sakyo-ku, Kyoto, Japan, 606-8507.

E-mail: kkwada@kuhp.kyoto-u.ac.jp

*Contributed equally to this work.

Published online Jul. 1, 2015.

COPYRIGHT © 2015 by the Society of Nuclear Medicine and Molecular Imaging, Inc.

caused higher ^{18}F -FDG accumulation possibly by upregulation of GLUT1 and at least partially by upregulating HIF-1 α induction under hypoxic conditions (10).

In a retrospective analysis of 51 primary CRCs, we previously reported that maximum standardized uptake value (SUV_{max}) was significantly higher in primary CRCs with mutated *KRAS* than in those with wild-type *KRAS* and that *KRAS* status could be predicted by ^{18}F -FDG PET/CT scans with an accuracy of 75% (8). The study by Kawada et al. (8) was the first clinical study showing the causal relationship between *KRAS* mutations and ^{18}F -FDG accumulation using ^{18}F -FDG PET/CT scans in a variety of cancers. There is also emerging evidence from other groups that ^{18}F -FDG accumulation reflects *KRAS* mutational status of CRC and non-small cell lung cancer (11–13). However, the clinical utility of these findings has been limited because endoscopic biopsy for *KRAS* mutational testing is safe and feasible only in primary CRC. It has not been investigated whether the similar relationship between *KRAS* mutations and ^{18}F -FDG accumulation exists in metastatic CRC. In particular, *KRAS* mutational testing derived from metastatic CRC samples is usually difficult because of limitations in sample availability. Therefore, the purpose of this study was to assess whether *KRAS* mutations are associated with ^{18}F -FDG accumulation in metastatic CRC and whether ^{18}F -FDG PET/CT scans can be used to predict the *KRAS* status of metastatic CRC. To our knowledge, this is the first clinical study showing a causal relationship between *KRAS* mutations and ^{18}F -FDG accumulation in metastatic CRC. Our study suggests that ^{18}F -FDG PET/CT scans may be useful to determine therapeutic strategies for CRC by predicting tumor response to anti-EGFR antibody therapy.

MATERIALS AND METHODS

Study Population

Sixty distant metastases were obtained from 38 CRC patients undergoing ^{18}F -FDG PET/CT scans before surgical resection at Kyoto University Hospital between April 2009 and March 2014. The diagnosis of metastatic CRC was confirmed by pathologic examination of surgical specimens. No patients received chemotherapy or radiation therapy 6 mo before ^{18}F -FDG PET/CT scans. Five distant metastases were excluded because they had the following non-tumor-related factors that can affect ^{18}F -FDG accumulation: uncontrolled diabetes mellitus—that is, a blood glucose level of 150 mg/dL or greater ($n = 4$)—and severe inflammation with C-reactive protein of 5.0 mg/dL or greater ($n = 1$). Finally, fifty-five distant metastases obtained from 35 CRC patients were included in this retrospective study. This study protocol was approved by the institutional review board of Kyoto University, Kyoto, Japan, and all patients provided their consent for data handling.

PET Imaging and Analysis

The methods for PET/CT imaging and quantitative analysis were detailed in our previous report (8). PET/CT scans were performed using a combined PET/CT scanner (Discovery ST Elite; GE Healthcare). This system integrates a PET scanner with a multidetector-row CT (16 detectors) scanner and permits the acquisition of coregistered CT and PET images in a single examination. Patients fasted for at least 4 h before ^{18}F -FDG administration. We checked patients' plasma glucose levels just before injecting ^{18}F -FDG, and there were no patients whose blood glucose level exceeded 150 mg/dL in this study. Data acquisition started approximately 60 min after the injection of a standard dose of 3.7 MBq/kg of ^{18}F -FDG. Initially, starting at the level of the upper thigh, the low-dose CT scans were obtained with the following parameters: 40–60 mA, 120 kV, 0.6-s tube rotation, and 3.75-mm section thickness. The CT images were acquired during

shallow breathing, and scanning included the area from the upper thigh to the skull. Immediately after CT, a PET emission scan was obtained with an acquisition time of 2–3 min per bed position. The total acquisition time was approximately 20 min. The CT data were used for attenuation correction, and images were reconstructed using the 3-dimensional iterative reconstruction algorithm called VUE Point Plus. For quantitative analysis, a board-certified radiologist/nuclear medicine physician assessed ^{18}F -FDG accumulation on a workstation (Advantage Workstation 4.4; GE Healthcare) by calculating the standardized uptake value (SUV) in the regions of interest placed over the suspected lesions and the normal liver. The SUV was calculated using the following formula: $\text{SUV} = C_{\text{dc}}/(D_i/W)$, where C_{dc} is the decay-corrected tracer tissue concentration (in Becquerel per gram); D_i , the injected dose (in Becquerel); and W , the patient's body weight (in grams). For evaluating metastatic CRC, the highest SUV in a metastatic tumor was taken as SUV_{max} .

KRAS Mutational Analysis

DNA was extracted from formalin-fixed, paraffin-embedded tumor tissue sections using the NucleoSpin DNA FFPE XS (Macherey-Nagel). *KRAS* exon 2 was amplified by polymerase chain reaction. The polymerase chain reaction products were directly sequenced using an ABI 3130 Genetic Analyzer (Applied Biosystems) according to the manufacturer's instruction.

Statistical Analysis

All values are expressed as mean \pm SD. Differences in SUV_{max} between mutated and wild-type *KRAS* were tested by a Mann-Whitney U test. The statistical significance of differences in Tables 1 and Table 2 was determined by the χ^2 test or Mann-Whitney U test. All analyses were 2-sided, and a P value of less than 0.05 was considered statistically significant. To determine the factors associated with *KRAS* mutational status in Table 3, multivariate logistic regression analysis was used, and factors with a P value of 0.10 or less were included in the model. The relationship between SUV_{max} and tumor size was determined by Pearson correlation coefficients. Statistical analyses were performed using SPSS software (version 11.50; SPSS Inc.).

RESULTS

Patient Population

The characteristics of patients and their metastatic tumors are presented in Table 4. The study group consisted of 55 distant metastases (liver, $n = 38$; lung, $n = 11$; distant lymph nodes, $n = 4$; peritoneal dissemination, $n = 2$) obtained from 35 CRC patients. All metastatic tumors were surgically resected within 30 d after ^{18}F -FDG PET/CT scans. *KRAS* mutations at codons 12 and 13 were found in 21 and 9 (38% and 16%, respectively) of the 55 metastatic tumors, whereas *KRAS* was wild-type in the remaining 25 samples (46%). SUV_{max} in the metastatic tumors ranged from 1.2 to 19.7 (5.9 ± 3.6).

Correlation Between SUV_{max} and *KRAS* Mutations

On the basis of *KRAS* mutational status, distant metastatic tumors were classified into 2 groups: tumors with wild-type *KRAS* ($n = 25$) and those with mutated *KRAS* ($n = 30$). Table 1 shows the results of the univariate analysis for each factor. SUV_{max} in the mutated *KRAS* group was not significantly different from that of wild-type *KRAS* group (6.3 ± 4.2 vs. 5.4 ± 2.6 , respectively; $P = 0.84$; Fig. 1C). However, the tumor size of the mutated *KRAS* group was smaller than that of the wild-type *KRAS* group, although not significantly different ($P = 0.06$). SUV_{max} can be underestimated because of partial-volume effect, particularly when tumor size is small (14). In fact, we found that SUV_{max}

TABLE 1
Univariate Analysis of Factors Associated with *KRAS* Status ($n = 55$)

Factor	Mutated <i>KRAS</i> ($n = 30$)	Wild-type <i>KRAS</i> ($n = 25$)	Univariate P
Mean age \pm SD (y)	65.4 \pm 12.2	62.8 \pm 8.1	0.20
Sex			1
Male	21	18	
Female	9	7	
Blood glucose			1
100	9	8	
≥ 100	21	17	
Mean C-reactive protein \pm SD	0.2 \pm 0.4	0.1 \pm 0.1	0.86
Carcinoembryonic antigen			1
5.0	16	13	
≥ 5.0	14	12	
Mean tumor size \pm SD (mm)	18.8 \pm 14.8	23.2 \pm 13.2	0.06
Mean SUV _{max} \pm SD	6.3 \pm 4.2	5.4 \pm 2.6	0.84

was significantly correlated with tumor size (Pearson correlation coefficient, $P = 0.006$; Supplemental Fig. 1A [supplemental materials are available at <http://jnm.snmjournals.org>]).

Therefore, we next examined the tumors larger than 10 mm to minimize bias produced by partial-volume effect. On the basis of *KRAS* status, tumors were classified into 2 groups: tumors with wild-type *KRAS* ($n = 23$) and those with mutated *KRAS* ($n = 19$). Table 2 shows the results of the univariate analysis for each factor. No significant differences were found between the 2 groups in terms of sex, blood glucose level, serum C-reactive protein level, serum carcinoembryonic antigen level, and tumor size. However, a significant difference in ^{18}F -FDG accumulation into the metastatic tumors was found between these 2 groups. Namely, SUV_{max} was significantly higher in the mutated *KRAS* group than in the wild-type *KRAS* group (8.3 ± 4.1 vs. 5.7 ± 2.4 , respectively; $P = 0.03$; Fig. 1D). Figure 1 shows typical ^{18}F -FDG PET/CT scans of the patients with mutated *KRAS* (Fig. 1A) and wild-type *KRAS*

(Fig. 1B). In the multivariate analysis including factors with a P value of 0.1 or less, only SUV_{max} remained to be significantly correlated with *KRAS* mutations (Table 3; odds ratio, 0.78; 95% confidence interval, 0.61–0.99; $P = 0.044$). We also confirmed that SUV_{max} was not correlated with tumor size in this setting (Pearson correlation coefficient, $P = 0.29$; Supplemental Fig. 1B), indicating that these results were independent of tumor size.

We then sought to determine the threshold for optimal differentiation between these 2 groups. Receiver-operating-characteristic curve analysis revealed that the highest accuracy (71.4%) was obtained with an SUV_{max} cutoff value of 6.0 and that the area under the curve was 0.70 (Supplemental Fig. 2). Sensitivity and specificity for the prediction of *KRAS* mutations were 68% (13/19) and 74% (17/23), respectively (positive predictive value, 68%, 13/19; negative predictive value, 74%, 17/23; accuracy, 71.4%, 30/42). These results suggested that ^{18}F -FDG PET/CT scans can be predictive of the *KRAS* status of metastatic CRC.

TABLE 2
Univariate Analysis of Factors Associated with *KRAS* Status in Tumors Larger Than 10 mm ($n = 42$)

Factor	Mutated <i>KRAS</i> ($n = 19$)	Wild-type <i>KRAS</i> ($n = 23$)	Univariate P
Mean age \pm SD (y)	67.1 \pm 12.4	62.0 \pm 8.1	0.05
Sex			1
Male	15	18	
Female	4	5	
Blood glucose			0.75
100	6	9	
≥ 100	13	14	
Mean C-reactive protein \pm SD	0.2 \pm 0.5	0.1 \pm 0.1	0.65
Carcinoembryonic antigen			0.54
5.0	7	11	
≥ 5.0	12	12	
Mean tumor size \pm SD (mm)	24.7 \pm 15.8	25.0 \pm 12.7	0.69
Mean SUV _{max} \pm SD	8.3 \pm 4.1	5.7 \pm 2.4	0.03

TABLE 3

Multivariate Analysis of *KRAS* Status in Metastatic CRC
(*n* = 42)

Factor	Odds ratio	95% confidence interval	<i>P</i>
Age	0.96	0.90 to 1.03	0.264
SUV _{max}	0.78	0.61 to 0.99	0.044

Concordance of *KRAS* Status Between Primary Tumor and Its Corresponding Metastatic Tumor

Of the 55 distant metastases in this study, 49 samples (89%) could be used to assess the association of *KRAS* status between paired primary and metastatic CRC samples. The aim was to investigate whether the *KRAS* status of primary CRC could be used as a surrogate for its corresponding metastatic CRC. Heterogeneity of *KRAS* status between a primary CRC and its corresponding metastases was found in 7 samples (14%; 7/49), which is consistent with the frequencies reported in previous studies (15). Namely, 3 metastatic CRCs had mutated *KRAS* in codon 13, whereas paired primary CRCs had wild-type *KRAS*; 2 metastatic CRCs had wild-type *KRAS*, whereas paired primary CRCs had mutated *KRAS* in codon 12; and 2 metastatic CRCs had mutated *KRAS* in codon 13, whereas paired primary CRCs had mutated *KRAS* in codon 12. In addition, discordant *KRAS* status also existed among metastatic CRCs from the same patient; 1 patient simultaneously had both codon 12–mutated and codon 13–mutated metastases.

DISCUSSION

The American Society of Clinical Oncology suggests that patients with metastatic CRC, having a *KRAS* mutation in codon 12 or 13, should not receive anti-EGFR antibody treatment (16). Although anti-EGFR antibody therapy has been established in CRC patients with wild-type *KRAS*, up to 50% of these patients do not respond to this therapy (17). Failure of EGFR antibody against CRC patients with wild-type *KRAS* may result from the intratumoral heterogeneity of *KRAS* status (3) and the discordant *KRAS* status between a primary CRC and its corresponding metastases (4,5). In fact, it remains unclear whether mutational testing of a primary CRC is sufficient to characterize its corresponding metastases. Some studies have found a high (>95%) concordance of *KRAS* mutations between primary CRCs and corresponding metastases (18,19), although others have reported a relatively low number (~70%) (3,4); the most commonly reported rate is approximately 90% (15). In addition, tumor tissue samples obtained by biopsy or surgery are necessary for mutational testing, but samples from metastatic tumors are usually difficult to access and may need invasive procedures. Therefore, alternative noninvasive strategies, such as ¹⁸F-FDG PET/CT scans, to predict mutation profile could be of value to overcome these limitations. We previously reported that ¹⁸F-FDG PET/CT scans can predict the *KRAS* status of primary CRC with an accuracy of 75% (8). In the present study, we have also shown that ¹⁸F-FDG PET/CT scans can predict the *KRAS* status of metastatic CRC with an accuracy of 71.4%, particularly in tumors larger than 10 mm. Although ¹⁸F-FDG PET/CT scans may not be enough for predicting *KRAS* status determined by mutational testing, they may reflect the macroscopic status of *KRAS* mutations. On the other hand, mutational testing of resected specimens may not reflect the macroscopic status of the whole tumor. Miles et al. recently reported that a combination of SUV_{max}, CT texture, and blood perfusion could

potentially improve the accuracy for the prediction of *KRAS* status of primary CRC (11). To optimize the clinical application of ¹⁸F-FDG PET/CT scans, future prospective studies should include a larger number of patients and use standardized protocols for ¹⁸F-FDG PET/CT acquisition and correction of partial-volume effect. In addition, together with more comprehensive genomic information, it is imperative to investigate whether ¹⁸F-FDG PET/CT scans can predict the actual response to anti-EGFR–based therapy and survival rates.

TABLE 4

Tumor Characteristics (55 Metastases Obtained from 35 Patients)

Characteristic	Patients	Metastases
Age (y)		
Mean ± SD	64 ± 10.5	
Range	43–91	
Sex		
Male	24	
Female	11	
Blood glucose		
Mean ± SD	106 ± 15	
Range	71–139	
C-reactive protein		
Mean ± SD	0.2 ± 0.3	
Range	0.0–2.3	
Carcinoembryonic antigen		
<5.0	29	
≥5.0	26	
Metastatic lesions		
Liver	38	
Lung	11	
Distant lymph nodes	4	
Peritoneal dissemination	2	
Timing		
Synchronous	12	
Metachronous	43	
No. of metastases/patient		
1	23	
2	8	
3	1	
4	2	
5	1	
Tumor size (mm)		
Mean ± SD	20.9 ± 14.2	
Range	7–81	
SUV_{max}		
Mean ± SD	5.9 ± 3.6	
Range	1.2–19.7	
<i>KRAS</i> status		
Mutated	30	
Wild-type	25	

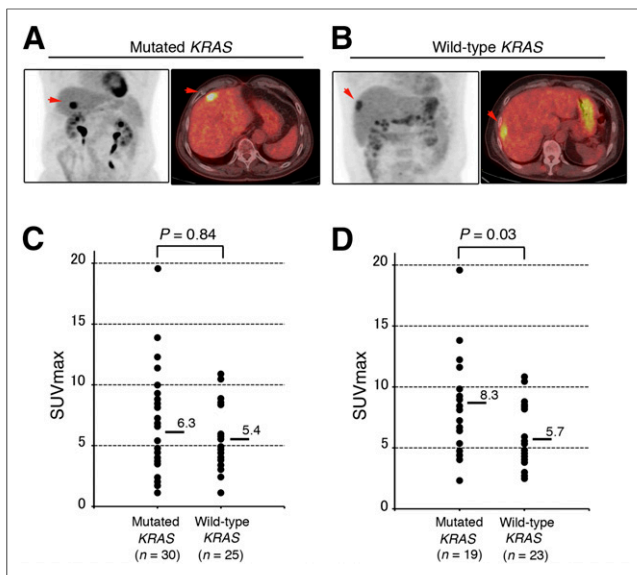


FIGURE 1. (A) A 78-y-old man had 1 liver metastasis (diameter, 23 mm) with mutated *KRAS*. ^{18}F -FDG PET/CT scans showed intense accumulation of ^{18}F -FDG in liver tumor (arrow; SUV, 8.3). (B) A 61-y-old man had 1 liver metastasis (diameter, 27 mm) with wild-type *KRAS*. ^{18}F -FDG PET/CT scans showed modest accumulation of ^{18}F -FDG in tumor (arrow; SUV, 4.5). (C) Analysis of SUV_{max} according to status of *KRAS*. With all liver tumors ($n = 55$), SUV_{max} of mutated *KRAS* group was not significantly different from that of wild-type *KRAS* group (6.3 ± 4.2 and 5.4 ± 2.6 , respectively; $P = 0.84$; exact Mann–Whitney U test). Means = bars. (D) With metastatic tumors larger than 10 mm ($n = 42$), SUV_{max} was significantly higher in mutated *KRAS* group than in wild-type *KRAS* group (8.3 ± 4.1 and 5.7 ± 2.4 , respectively; $P = 0.03$; exact Mann–Whitney U test). Means = bars.

^{18}F -FDG PET/CT scans are used to evaluate glucose metabolism by measuring uptake of ^{18}F -FDG, a glucose analog. It was reported that metastatic liver CRC tumors more than 10 mm could be detected by ^{18}F -FDG PET/CT scans with a sensitivity of approximately 97%, whereas those with a diameter of 10 mm or smaller could be detected with a sensitivity of approximately 45% (20). The molecular mechanisms causing upregulation of glucose metabolism in CRC have not yet been investigated. Yun et al. previously reported that, under normoxic condition, the increase in GLUT1 expression and glucose uptake was critically dependent on *KRAS* mutations in CRC cell lines (7). In vitro assays using CRC cell lines indicated that *KRAS* mutations caused about a 2.0-fold increase in glucose uptake by upregulation of GLUT1 expression (7). We previously conducted a retrospective analysis of 51 primary CRCs and found that *KRAS* mutations significantly increased ^{18}F -FDG accumulation possibly through upregulation of GLUT1 expression (8), which indicates that ^{18}F -FDG accumulation may reflect a genetic mutation—that is, *KRAS*. Primary CRCs with mutated *KRAS* showed about a 1.5-fold increase in SUV_{max} when compared with those with wild-type *KRAS* ($P < 0.01$). There is also emerging evidence from other groups that ^{18}F -FDG accumulation reflects the *KRAS* mutational status of CRC and non-small cell lung cancer (11–13). In this clinical study, we have shown that, in metastatic CRC tumors larger than 10 mm, mutated *KRAS* showed about a 1.45-fold increase in SUV_{max} compared with wild-type *KRAS* ($P < 0.05$; Fig. 1D; Table 2). To our knowledge, this is the first study to analyze the association between *KRAS* status and ^{18}F -FDG accumulation in metastatic CRC.

The mechanisms underlying ^{18}F -FDG accumulation into cancer tissues are more complex. These factors include tumor-related (e.g., tumor size and hypoxia) and non-tumor-related components (e.g., diabetes mellitus, inflammation, and chemotherapy) (21–23). It was reported that SUVs of liver metastases in CRC patients who received chemotherapy within 3 mo of hepatic surgery were lower than those who did not receive chemotherapy within 3 mo of surgery (24). In this study, patients with uncontrolled diabetes mellitus and severe inflammation were not included. Moreover, patients who received chemotherapy 6 mo before ^{18}F -FDG PET/CT scans were also excluded. HIF-1 α has been shown to regulate transcription of GLUT1 in hypoxic conditions (25). When CRC cells were treated under hypoxic conditions, mutated *KRAS* enhanced the translation of HIF-1 α through the phosphoinositide 3-kinase pathway (26). We recently reported that CRC cells with mutated *KRAS* increased ^{18}F -FDG accumulation by upregulating GLUT1 and at least partially by upregulating HIF-1 α induction under hypoxic conditions (10). In this study, we investigated a possible association between *KRAS* status and HIF-1 α expression by immunohistochemical analysis and found that HIF-1 α did not correlate with *KRAS* status in metastatic CRC (data not shown). Our previous studies on primary CRC showed a significant correlation between HIF-1 α and *KRAS* status (10). One possible reason for this discrepancy may be the difference in tumor size (primary CRC, 47.9 ± 20 vs. metastatic CRC, 20.9 ± 14.2 mm; $P < 0.01$). Another reason could be the difference of microenvironment between the colon and its metastatic sites.

CONCLUSION

This study is a relatively small, retrospective analysis, but it highlights the fact that ^{18}F -FDG accumulation in metastatic CRC with mutated *KRAS* is significantly higher than that with wild-type *KRAS*, when the tumors are larger than 10 mm. Although a larger number of patients are needed to confirm our findings, these results indicate that ^{18}F -FDG PET/CT scans could be useful in the prediction of *KRAS* mutational status.

DISCLOSURE

The costs of publication of this article were defrayed in part by the payment of page charges. Therefore, and solely to indicate this fact, this article is hereby marked “advertisement” in accordance with 18 USC section 1734. This work was supported by grants from the Ministry of Education, Culture, Sports, Science and Technology of Japan. No other potential conflict of interest relevant to this article was reported.

REFERENCES

1. Karapetis CS, Khambata-Ford S, Jonker DJ, et al. K-ras mutations and benefit from cetuximab in advanced colorectal cancer. *N Engl J Med*. 2008;359:1757–1765.
2. Amado RG, Wolf M, Peeters M, et al. Wild-type *KRAS* is required for panitumumab efficacy in patients with metastatic colorectal cancer. *J Clin Oncol*. 2008;26:1626–1634.
3. Baldus SE, Schaefer K-L, Engers R, Hartleb D, Stoecklein NH, Gabbert HE. Prevalence and heterogeneity of *KRAS*, *BRAF*, and *PIK3CA* mutations in primary colorectal adenocarcinomas and their corresponding metastases. *Clin Cancer Res*. 2010;16:790–799.
4. Albanese I, Scibetta AG, Migliavacca M, et al. Heterogeneity within and between primary colorectal carcinomas and matched metastases as revealed by analysis of Ki-ras and p53 mutations. *Biochem Biophys Res Commun*. 2004;325:784–791.

5. Molinari F, Martin V, Saletti P, et al. Differing deregulation of EGFR and downstream proteins in primary colorectal cancer and related metastatic sites may be clinically relevant. *Br J Cancer*. 2009;100:1087–1094.
6. Jadvar H, Alavi A, Gambhir SS. ¹⁸F-FDG uptake in lung, breast, and colon cancers: molecular biology correlates and disease characterization. *J Nucl Med*. 2009;50:1820–1827.
7. Yun J, Rago C, Cheong I, et al. Glucose deprivation contributes to the development of KRAS pathway mutations in tumor cells. *Science*. 2009;325:1555–1559.
8. Kawada K, Nakamoto Y, Kawada M, et al. Relationship between ¹⁸F-fluorodeoxyglucose accumulation and KRAS/BRAF mutations in colorectal cancer. *Clin Cancer Res*. 2012;18:1696–1703.
9. Semenza GL. HIF-1 mediates metabolic responses to intratumoral hypoxia and oncogenic mutations. *J Clin Invest*. 2013;123:3664–3671.
10. Iwamoto M, Kawada K, Nakamoto Y, et al. Regulation of ¹⁸F-FDG accumulation in colorectal cancer cells with mutated KRAS. *J Nucl Med*. 2014;55:2038–2044.
11. Miles KA, Ganeshan B, Rodriguez-Justo M, et al. Multifunctional imaging signature for V-KI-RAS2 Kirsten rat sarcoma viral oncogene homolog (KRAS) mutations in colorectal cancer. *J Nucl Med*. 2014;55:386–391.
12. Chen SW, Chiang HC, Chen WT, et al. Correlation between PET/CT parameters and KRAS expression in colorectal cancer. *Clin Nucl Med*. 2014;39:685–689.
13. Caicedo C, Garcia-Velloso MJ, Lozano MD, et al. Role of [¹⁸F]FDG PET in prediction of KRAS and EGFR mutation status in patients with advanced non-small-cell lung cancer. *Eur J Nucl Med Mol Imaging*. 2014;41:2058–2065.
14. Soret M, Bacharach SL, Buvat I. Partial-volume effect in PET tumor imaging. *J Nucl Med*. 2007;48:932–945.
15. Baas JM, Krens LL, Guchelaar HJ, Morreau H, Gelderblom H. Concordance of predictive markers for EGFR inhibitors in primary tumors and metastases in colorectal cancer: a review. *Oncologist*. 2011;16:1239–1249.
16. Allegra CJ, Jessup JM, Somerfield MR, et al. American Society of Clinical Oncology provisional clinical opinion: testing for KRAS gene mutations in patients with metastatic colorectal carcinoma to predict response to anti-epidermal growth factor receptor monoclonal antibody therapy. *J Clin Oncol*. 2009;27:2091–2096.
17. Lièvre A, Bachet JB, Boige V, et al. KRAS mutations as an independent prognostic factor in patients with advanced colorectal cancer treated with cetuximab. *J Clin Oncol*. 2008;26:374–379.
18. Etienne-Grimaldi MC, Formento JL, Francoual M, et al. K-ras mutations and treatment outcome in colorectal cancer patients receiving exclusive fluoropyrimidine therapy. *Clin Cancer Res*. 2008;14:4830–4835.
19. Santini D, Loupakis F, Vincenzi B, et al. High concordance of KRAS status between primary colorectal tumors and related metastatic sites: implications for clinical practice. *Oncologist*. 2008;13:1270–1275.
20. Suenaga Y, Kitajima K, Aoki H, et al. Respiratory-gated ¹⁸F-FDG PET/CT for the diagnosis of liver metastasis. *Eur J Radiol*. 2013;82:1696–1701.
21. Pauwels EK, Ribeiro MJ, Stoot JH, McCready VR, Bourguignon M, Mazière B. FDG accumulation and tumor biology. *Nucl Med Biol*. 1998;25:317–322.
22. Gillies RJ, Robey I, Gatenby RA. Causes and consequences of increased glucose metabolism of cancers. *J Nucl Med*. 2008;49:24S–42S.
23. Plathow C, Weber WA. Tumor cell metabolism imaging. *J Nucl Med*. 2008;49:43S–63S.
24. Akhurst T, Kates TJ, Mazumdar M, et al. Recent chemotherapy reduces the sensitivity of [¹⁸F]fluorodeoxyglucose positron emission tomography in the detection of colorectal metastases. *J Clin Oncol*. 2005;23:8713–8716.
25. Chen C, Pore N, Behrooz A, Ismail-Beigi F, Maity A. Regulation of glut1 mRNA by hypoxia-inducible factor-1: interaction between H-ras and hypoxia. *J Biol Chem*. 2001;276:9519–9525.
26. Kikuchi H, Pino MS, Zeng M, Shirasawa S, Chung DC. Oncogenic KRAS and BRAF differentially regulate hypoxia-inducible factor-1 α and -2 α in colon cancer. *Cancer Res*. 2009;69:8499–8506.